A Design Document for the Neutrino-Induced Neutron Pile Concept

P. S. Barbeau, J. I. Collar, Y. Efremenko, D. Hornback,
J. Newby, D. Reyna, G. C. Rich, K. Scholberg

August 6, 2014

The purpose of this document is describe a concept for a simple, compact and cheap detector that can be used at the Spallation Neutron Source (SNS) to measure neutrino-nucleus cross-sections that can lead to the emission of neutrons. Such neutrons, produced in shielding and construction materials have the potential to contribute significantly to the background in the planned COHERENT neutrino-nucleus scattering experiments. There is significant theoretical uncertainty in the cross-sections, which suggests a measurement of the process would have value in the theory community. The cross-section is also important for the HALO collaboration, as it is the mechanism for detecting neutrinos from supernovae.

1 The Baseline Pile Design

The primary goal of this effort is to obtain a measurement of the neutron production in Pb shielding material in the presence of the high flux of high energy neutrinos at the SNS. It is then possible to infer with some confidence the individual (neutron emitting) charge-current and neutral current cross-sections. The desire for a quick result is one of the primary drivers of this design. This is subject to the complexity of the design, the availability of the deployment location, the availability of resources and the level to which the engineering safety review will need to delve.

A baseline[1] pile concept has been developed that incorporates a mass of natural Pb, instrumented with PSD capable liquid scintillator detectors. An image of this can be seen in figure 1. Starting at the innermost level, the baseline pile includes ∼660 kg of lead. The main components are:

- The lead can be cast into a single shape if needed for the purposes of stability and health safety. It is likely easier to fabricate at Duke/TUNL[2] if it is cast in 5 pieces, shown in figure 1: a16"x16"x6" base with four 8"x8"x10" collars with hollow cylindrical centers that house the detectors.
- Four PSD capable liquid scintillator detectors.
- A ∼95% efficient muon veto to eliminate neutrons produced from cosmic rays in the lead.
- A 4π neutron shield composed of Waterbricks. The bricks are stackable, and can be aligned with posts that can be passed through each layer in order to improve stability. The holes can be seen in figure 1

[1] In this context, the term baseline is used to describe a conceptual starting point for the design. It may not be physically possible, or feasible, but improvements can be conceived that are able to address this.

[2] Here we take advantage of the capability and experience of the Duke/TUNL instrument shop for casting Pb into arbitrary shapes. We also plan to use some of the more than 80 tons of Pb available at no cost to TUNL.

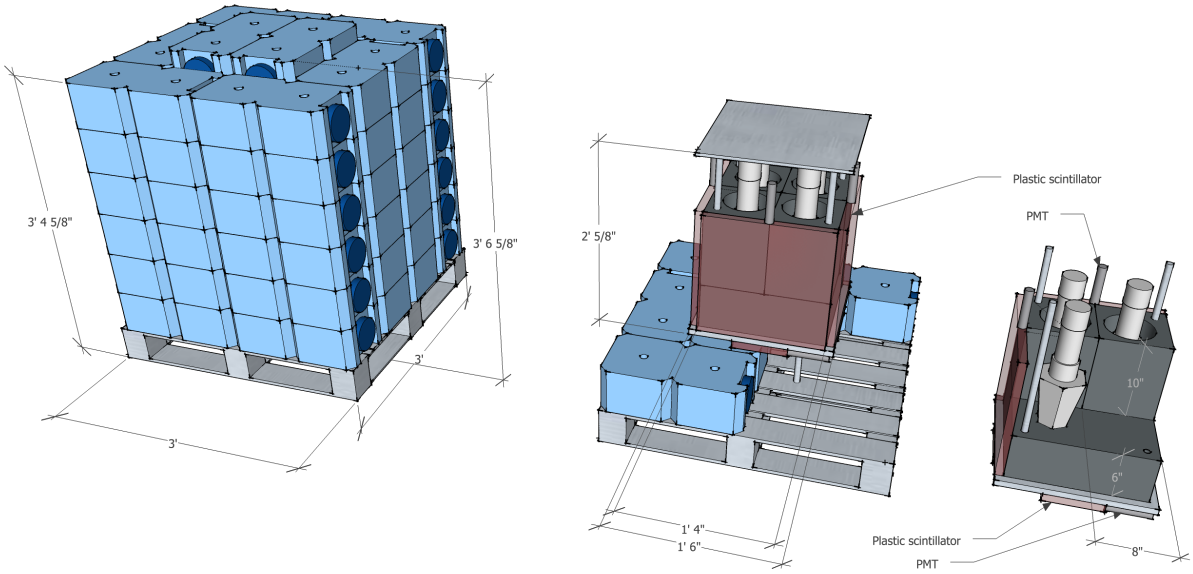

Figure 1: Conceptual drawing of pile v 1.0. Each pile is limited to a single 36" x 36" pallet for ease of transport.

- High capacity aluminum pallet (4,000 lbs dynamic capacity) with a 36"x36" footprint.

It should be noted that all materials where chosen in order to minimize the fire loading in the corridor and so that the size of the pile did not exceed 36" on a side. In principle, once disconnected from the electronics, each pile can be moved as a unit on a single pallet, possibly without any construction on site. This has major advantages from the point of view of safety and materials handling at the SNS.

Geometries other than this baseline design are also being studied in an attempt to increase detection efficiencies. This typically involves higher costs. With higher interaction rates, measurements of the neutrino multiplicity and energy spectrum, or using other target materials, can easily be envisioned. The modular and cheap design opens the door to studying multiple materials in parallel, or measuring the neutrino flux at multiple locations.

1.1 The Simulation

1.1.1 Efficiency

The pile geometry has been simulated using the MCNP-Polimi framework. This particular version of MCNP allows the full analog tracking of neutrons, photons and electron interactions. We limit this simulation to neutron and photon mode only. A post-processing code identifies interactions in the liquid scintillators, reproduces scintillator responses as a function of the energy deposited and of identify of each individual recoil. For example, the scintillation response of hydrogen recoils is $\sim 1/10^{th}$ that of electrons, and about a factor of 10 larger than the same energy carbon recoils, though the full behavior has some energy dependence. Two energy thresholds were tested (30 keVee

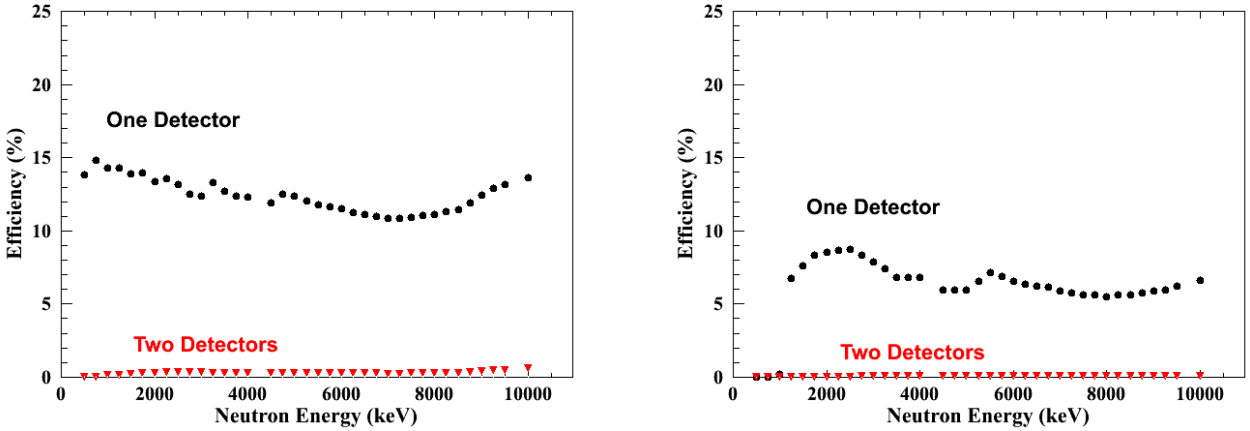

Figure 2: Black dots indicate the neutron detection efficiency curves for the simulated pile geometry and detectors with 30 keVee PSD thresholds (left) and 100 keVee PSD thresholds (right). Red triangles indicate the efficiency for a single neutron to give rise to two valid neutron signals.

and 100 keVee) representing two hypothetical energies below which the n-γ PSD capability begins to fail.

Within the simulation, we label valid neutron detection events when a neutron scatters in at least one liquid scintillator cell with sufficient energy to surpass the chosen 30 (100) keVee threshold. In addition, there cannot be a a gamma interaction within that same cell for it to be considered a clean hit, as such an interaction has the potential to confuse the PSD algorithms. Such a phenomenon is conveniently rare.

It is important to point out that the simulation does not attempt to incorporate detector effects such as light collection efficiencies or PSD capabilities. Such a simulation is a tall order, and would need to be matched and verified against actual detector capabilities. In lieu of this, we assume in these preliminary studies only that the PSD capabilities of the detectors presented here are able to efficiency separate neutron and gamma events for energies above the 30 or 100 keVee thresholds.

Efficiency curves for single neutrons were generated by producing isotropic, mono-energetic neutrons uniformly distributed throughout the Pb target. The effect of the energy thresholds is evident. Importantly, the neutron detection efficiency is, to a large degree, flat as a function of energy. A notable exception to this is the increase at energies >7 MeV, which is due to the onset of the (n, 2n) cross-section in lead. Also shown is the probability that a single neutron event gives rise to multiple valid liquid scintillator cell events. The rate is unsurprisingly low, though it also indicates an increased efficiency for energies >7 MeV, as one would expect.

1.1.2 Signal vs Background

Given the compact and easily transportable nature of the pile, it is hoped that a deployment in the basement hallway at position c5 can be achieved. For this location, seen in figure 3, it is assumed that an overburden of 8 m.w.e. is achieved and that the mercury target is at a distance of 20 m. This needs to be confirmed

The full simulation incorporates several sources of signal and background sources in order to estimate the experimental sensitivity of a deployment. The components are:

- The primary signal is the charge-current reaction: ^{208}Pb(ν_e, e)^{208}Bi + neutrons, which arrives

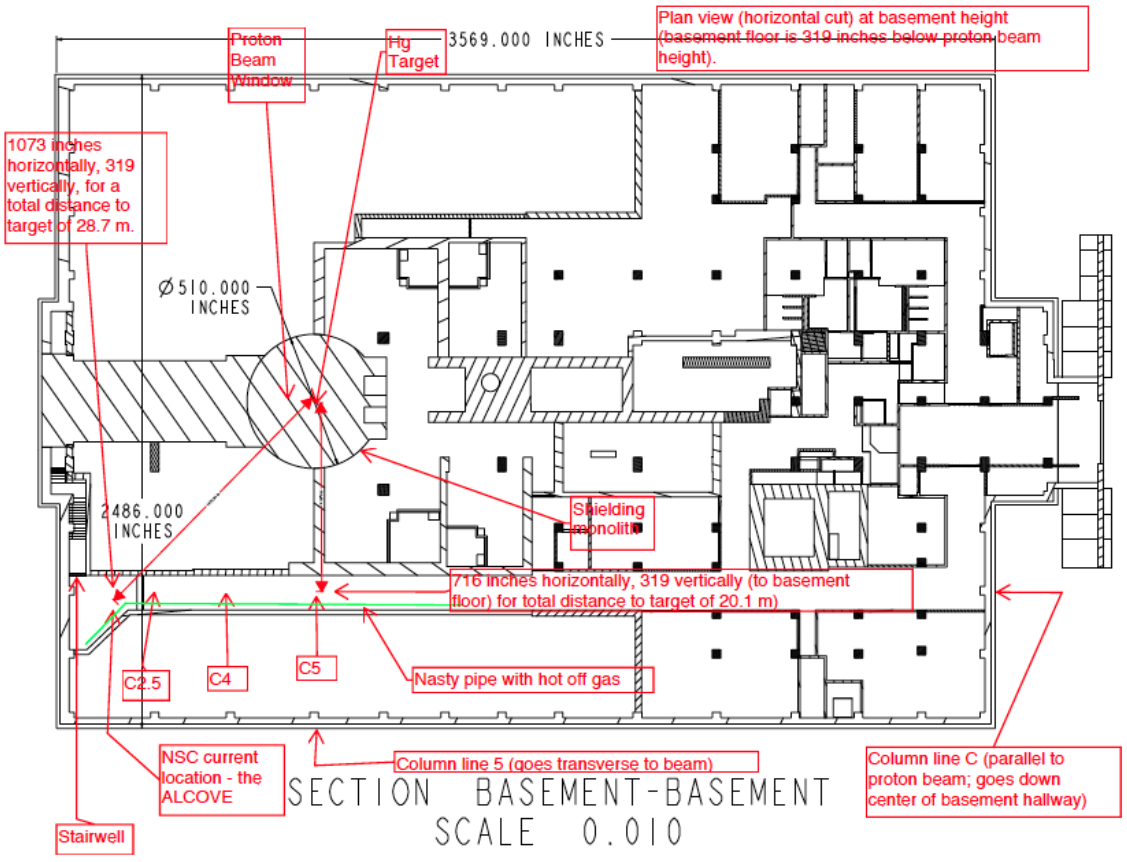

Figure 3: A schematic of the underground level of the SNS target building. It is hoped that position c5 will be available for experiments with the pile.

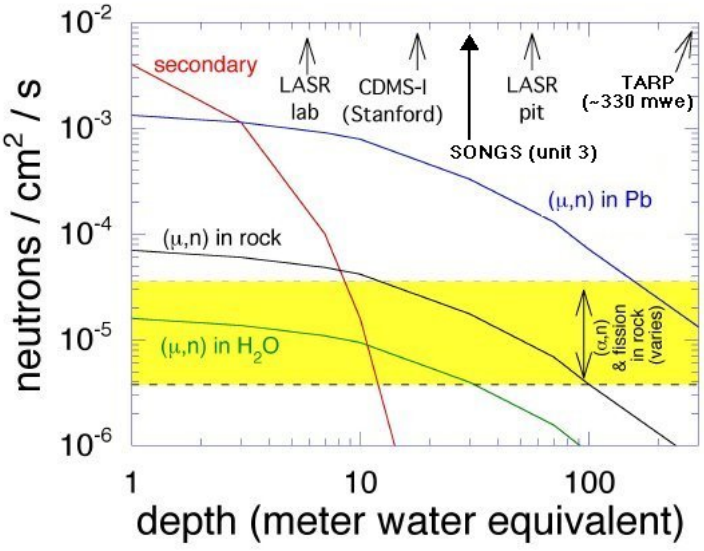

Figure 4: Neutron flux versus overburden from a range of sources. At 8 m.w.e., the cosmic secondary neutron flux is larger than both the (μ, n) and the (α, n) + fission neutrons in the rock. These two sub-dominant contributions have not been incorporated in the simulation as of yet. The (μ, n) in the H_2O have a larger flux inside the water shield because the water shield is designed to attenuate neutrons from the local environment. This is not true for the neutrons produced in the water shield itself.

delayed with respect to the beam spill, following the characteristic decay of the muon.

- The neutral current scattering of ^{208}Pb(ν_μ, ν_μ)Pb + neutrons, which is estimated to be an order of magnitude lower than the charge-current reaction, and arrives prompt with the beam spill.
- The neutral current scattering of ^{208}Pb($\bar{\nu_\mu}$, $\bar{\nu_\mu}$)Pb + neutrons, which is also estimated to be an order of magnitude lower than the charge-current reaction and also arrives delayed with respect to the beam spill.
- The neutral current scattering of ^{208}Pb($\bar{\nu_e}$, $\bar{\nu_e}$)Pb + neutrons, which is also estimated to be an order of magnitude lower than the charge-current reaction and also arrives delayed with respect to the beam spill.
- The primary background from μ-induced neutrons on Pb, accounting for the muon flux reduction due to 8 m.w.e. overburden and a 95% efficient muon veto.
- A secondary background from μ-induced neutrons on the H_2O shielding, accounting for the muon flux reduction due to 8 m.w.e. overburden. It is conservatively assumed that no reduction is achieved due to the operation of the muon veto.
- Cosmic secondary neutrons, accounting for the significant reduction incurred due to the estimated 8 m.w.e. overburden.

The muon induced neutron energy spectra were assumed to have evaporative and direct emission components. The spectrum used for the lead can be seen in figure 6. The energy spectrum for

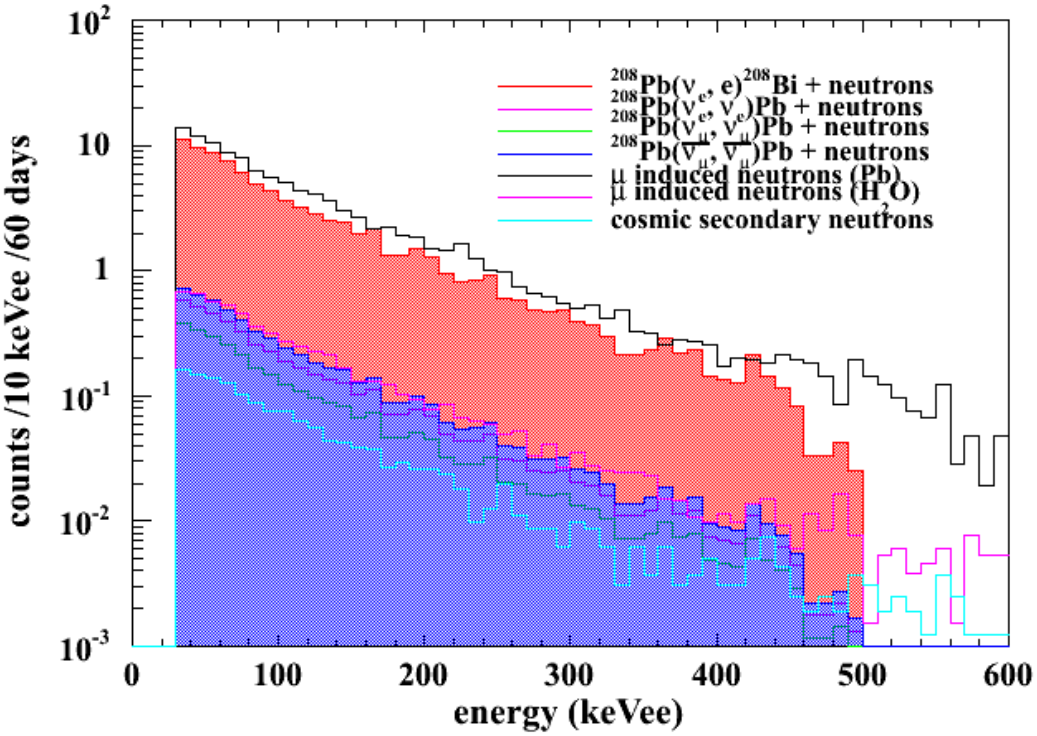

Figure 5: Signal and background energy deposition spectra for neutron events in the liquid scintillator detectors for a pile located at 8 m.w.e. and 20 m from the SNS target. The muon induced neutrons produced on Pb have been reduced as a result of 95% muon veto incorporated in the pile design.

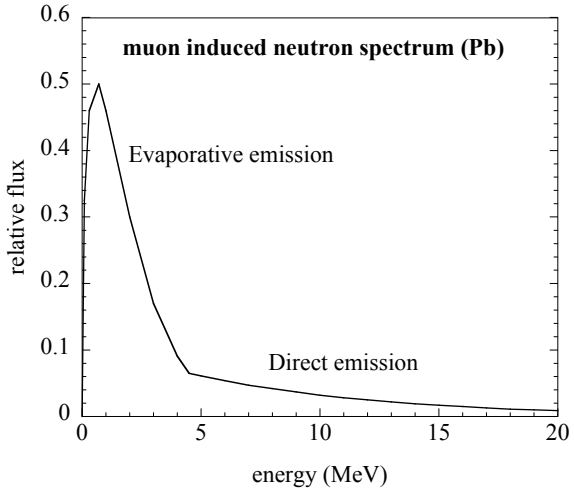

Figure 6: Neutron energy spectrum used in the simulation for muon induced neutrons in the Pb.

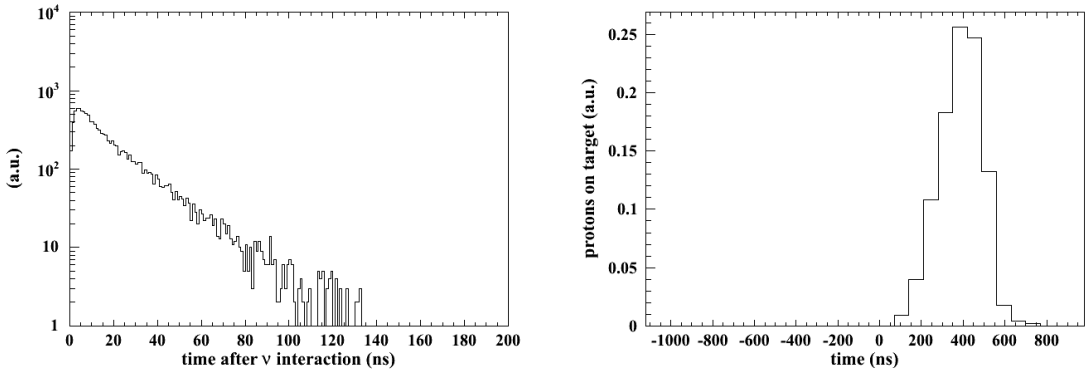

Figure 7: Left: Arrival time of the first above threshold signal detected after a neutrino induced neutron event in the Pb pile. Clearly, neutron straggling times are unlikely to be an issue for this effort. Right: Time structure of the proton beam.

the neutrino-induced neutrons on Pb was assumed to have an evaporative spectrum with a 5 MeV cutoff. This is only an approximation. One desired outcome of this measurement would be a high-statistics measurement of the neutron energy spectrum. The Hess spectrum was used as the initial energies of the cosmic secondary neutrons.

1.1.3 Timing

The combined speed of the fast neutrons with the fast liquid scintillator detectors allows us to take some advantage of the timing characteristics of the beam in order to identify signals and reduce backgrounds.

The arrival time of the first above threshold signal due to neutrino induced neutron events, as propagated by the MCNP-Polimi simulation, can be seen in figure 7. The arrival time structure is significantly faster than the beam structure, and is comparable to the response time of the liquid scintillator.

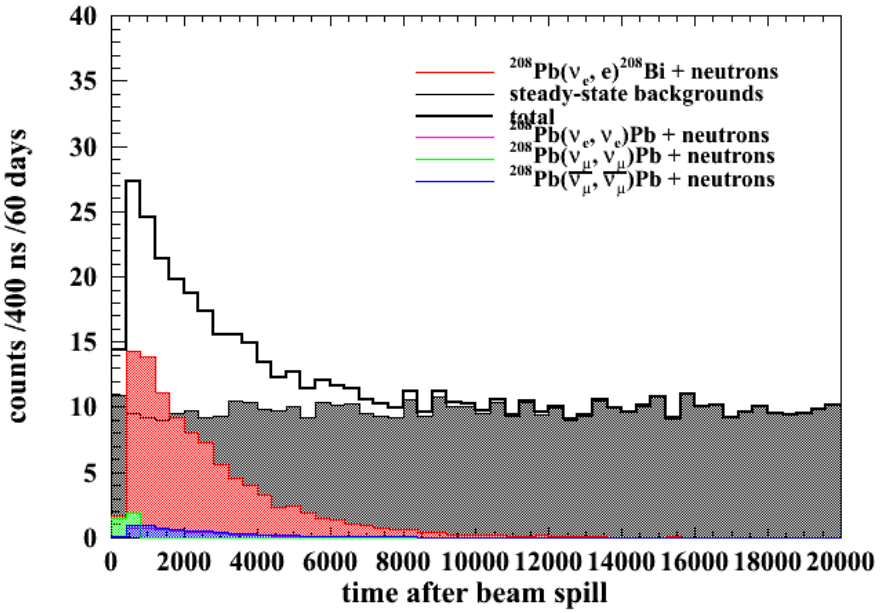

Figure 8: Time structure of the neutrino-induced neutron signals from both charge-current and neutral current interactions is shown. Also shown are the stead-state backgrounds, dominated by muon-induced neutrons in the Pb. A 5μs timing window cut after time-zero is used in the simulation to further reduce the effect of backgrounds. Notice that given a large enough exposure, a study of the prompt neutral current reaction could also potentially be studied. A 60 day exposure was used here.

This arrival time has been convolved with the timing structure of the proton beam pulse in order to study the timing-discrimination capabilities of the pile detector. The effect of this convolution can be seen in figure 8for a detector with a 30 keVee threshold for PSD, for a 60 day exposure. A further background reduction, seen in the energy spectra in figure 9, is achieved by implementing a 5 μs cut on the arrival of the first detectable neutron after the beam pulse.

1.2 Significance

The expected signal is shown in figure 9 for both 30 and 100 keVee thresholds, after all background timing and veto cuts have been applied.

If a 30 keVee threshold is achieved, and a single pile is deployed for 60 days at the SNS (assuming nominal SNS operating conditions), 100 signal events are expected on top of 122 background events (0.15 counts/kg Pb /60 days). This would result in a $\sim$6 σ observation of the total neutron producing cross-section as predicted by SNOWGLOBES. Should the detectors only achieve a threshold of 100 keVee, then a $\sim$4 σ result could be expected (0.06 counts/kg Pb /60 days).

Given the fact that neutrons from muons interacting in the Pb are the dominant background contributor, simple scaling arguments can easily be used to estimate the sensitivity for different muon veto efficiencies.

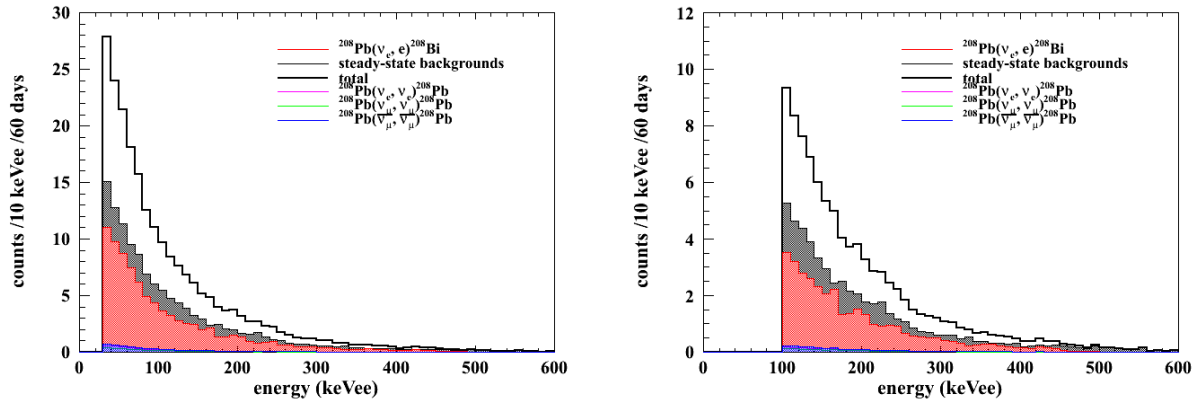

Figure 9: Signal and backgrounds for a deployment of single, 30 keVee (Left) and 100 keVee (Right) threshold piles at 8 m.w.e. and 20 m from target for 60 days.

1.2.1 Effect of the 2n/1n Emission Ratio

In addition to the theoretical uncertainty on the overall cross-section for neutrino-induced neutron production on Pb, the relative number of single and double neutron emission is also not very well predicted. The relationship between 2n and 1n events is strongly dictated by the underlying nuclear structure as well as the energy of the interacting neutrinos. It is interesting to see if the baseline pile design can to say anything about this ratio, as well as whether any uncertainty in this ratio has any impact on the total cross-section that is inferred by a measured rate of neutrons.

The baseline pile has a relatively low efficiency for the detection of neutrons emitted from the Pb (∼8–13%, depending on the detector thresholds and neutron energies). Thus, it is unlikely that by measuring the 2n/1n ratio of detected neutrons that there will be any significant sensitivity to the true 2n/1n ratio.

For the purposes of this analysis, the 2n/1n ratio from the SNOWGLOBES software package is assumed (∼0.54) as the nominal theory. The breakdown is as follows:

By varying the *true* ratio, and studying the measured 2n/1n ration, an estimate can be made for the sensitivity of a pile to this value. Figure 10 shows this relationship between the *true* 2n/1n ratio and the measured ratio. Due to the low efficiencies involved, even a measurement of the 2n/1n detected ratio with 20 times the exposure of the expected single pile, 60 day run, will have little to no impact on our understanding of the *true* 2n/1n ratio. This is shown by the 1σ bands in figure 10.

The next question to ask is to what extent the uncertainty in the *true* 2n/1n ratio has on our detection efficiency. Any change in the detection efficiency will have a direct impact on the inferred cross-section for the process. A similar study as above was performed and is shown in figure 11.

As can be seen, a 70% uncertainty on the *true* 2n/1n ratio will only have a an estimated ∼8% impact on the inferred cross-section determination. This is likely due to the nature of the detection algorithm used. An event is consider a valid neutrino-induced neutron production candidate if there is at least one detector cell that has seen a clean neutron signal above the PSD detection threshold. This metric , combined with the low detection efficiency for a single neutron, effectively diminishes the impact of the *true* 2n/1n ratio. It would be interesting to study the range of theoretically predicted ratios to determine if they already provide stronger constraints to this measurement. Also shown in the figure are the 1σ bands from a factor of 20 exposure increase, and their projected

Table 1: SNOW GLOBES output for the total neutron production cross-sections on ^{208}Pb for the SNS neutrino spectrum.

Total NC	13.32%
Total ν_e CC	86.68%
Total ν_e CC 1n	55.21%
Total ν_e CC 2n	31.47%
Total 1n	64.62%
Total 2n	35.38%
Total NC ν 1n	5.69%
Total NC ν 2n	1.83%
Total NC ν_e 1n	3.17%
Total NC ν_e 2n	1.39%
Total NC ν_μ 1n	2.52%
Total NC ν_μ 2n	0.44%
Total NC $\bar{\nu}$ 1n	3.71%
Total NC $\bar{\nu}$ 2n	2.08%

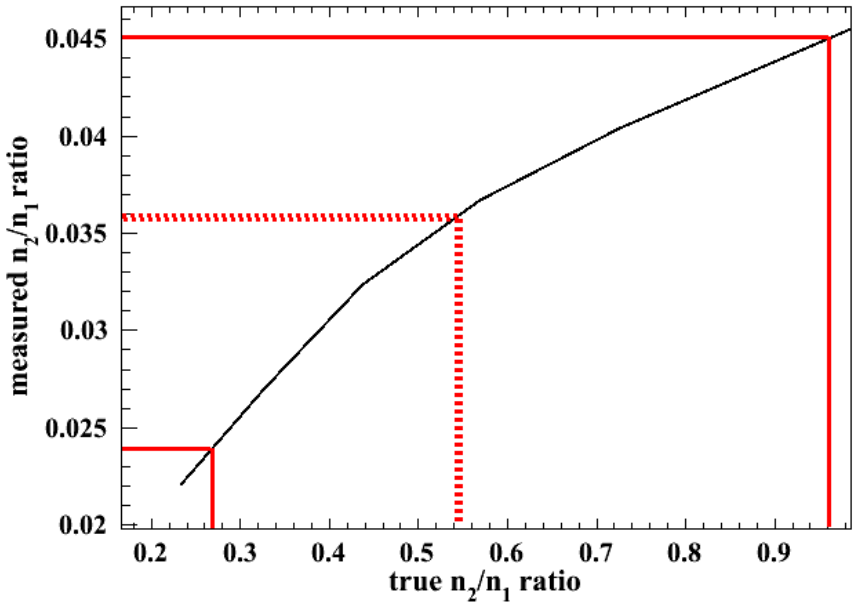

Figure 10: Relationship between the *true* 2n/1n ratio, and the ratio that is observed in the pile. There is a significant suppression of this ratio due to the low 8–13% efficiency of the pile for detecting neutrons produced in the Pb. The red bands indicate the central value, and 1 σ uncertainty for a measured 2n/1n ratio, assuming a factor of 20 increase in exposure (over a 1 pile, 60 day run). The resulting measurement provides little insight into the *true* ratio.

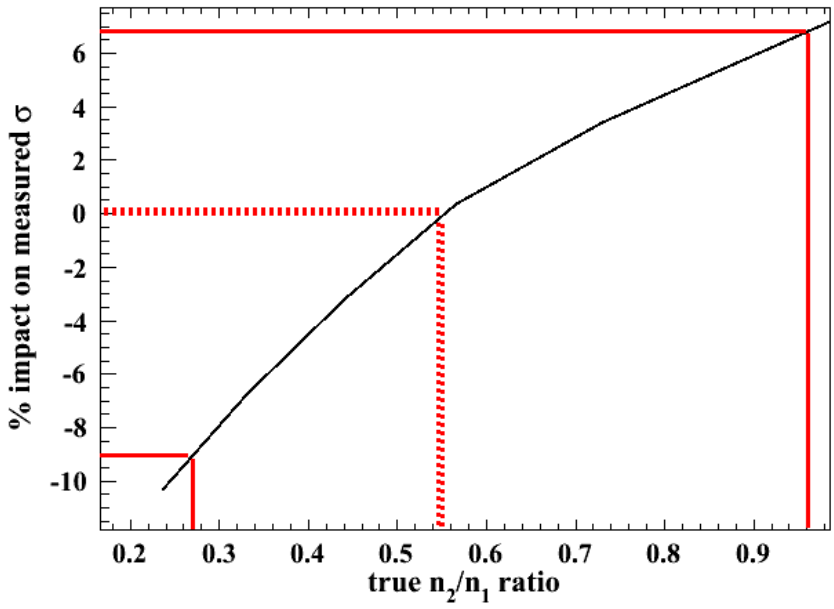

Figure 11: Relationship between the *true* 2n/1n ratio and it's impact on the measured total neutrino induced cross-section, assuming the production ratios from SNOWGLOBES are used.

impact on the inferred cross-section. Given that the neutrino flux uncertainty is estimated at ∼10%, and the signal is expected to be contaminated by neutral current cross-sections at the ∼10% level, it seems unnecessary to attempt to reduce this systematic uncertainty by studying a very difficult to measure 2n/1n ratio in a single pile.

1.3 Baseline Design Cost Breakdown

A crude estimate for the construction of the baseline design is included below. Significant cost-savings can be envisioned, especially if we fabricate out own liquid scintillator cells.[3] In large part, the cost will be driven by the quantity of PMTs that are used; an important tradeoff as it is important to have high light collection efficiency in order to push the PSD threshold to low energies.

2 Designs with More LS Cells

We are also considering modifying the design in an attempt to increase the efficiency for detecting neutrons, for reducing the overall cost, and also potentially eliminating the need for a muon veto. Two such drawings can be seen in figure 12. Considering the extremely large loads that the pallets can handle, we are also estimating the impact of including a second 6" block on Pb at the bottom of the pile on the projected sensitivity of the effort.

A "spherical-cow" study was performed in order to help eliminate what might be the most efficient ratio of liquid scintillator size to the mass of lead target that surrounds it. Liquid scintillator cells of 2 and 4 inches diameter were simulated. Neutrons were produced in lead spherical lead

[3]For example, J. I. Collar has obtained a quote for 5 gallons of BC501a at $1,145.00.

Table 2: Cost breakdown estimate for the Baseline Pile design.

Item	quantity	unit cost	cost
Galvanized steel pallet (4,000 lbs dyn. cap.)	1	$169.36	$169.36
1" PMTs (muon veto) ETL 9111B	6	$410.00	$2,460.00
ETL C673 voltage dividers	6	$92.00	$552.00
Muon Veto, 16" x 22" x 1", side panel, EJ-200	4	$420.00	$1,840.00
Muon Veto, bottom $\sim$ 1"x18"x18"	1	$420.00	$420.00
Pb cast to shape (material & fab. cost)	1	$600.00	$600.00
M510-50x50-8/301 LS Det. (Eljen)	4	$6,521.00	$26,084.00
Roof plate, 3/8" x 18" x 18" Al 7075-T6	1	$217.08	$217.08
Base plate, 3/4" x 18" x 18" SS	1	$826.20	$826.20
Inner support posts, 28", 3/4" OD, 1/4" wall th 316 SS	4	$166.60	$666.40
Base support posts, 7 1/2", 1" OD, 316 SS	1	$420.00	$420.00
Waterbricks	40	$17.49	$699.60
Digiters & Electronics (Duke/ORNL?)	-	-	-
total construction and material costs			$34,954.64
cost /ν /1 yr			$56.27

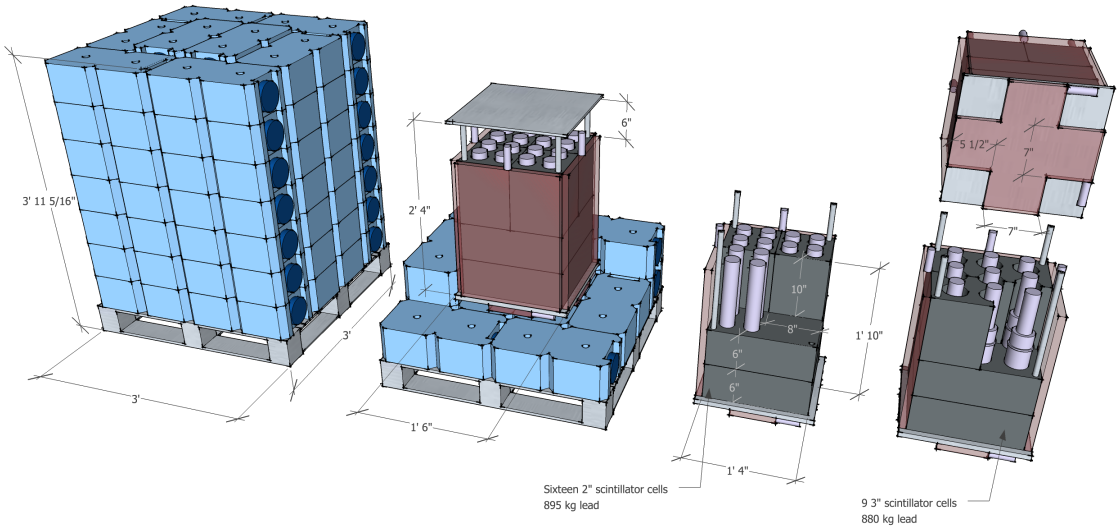

Figure 12: Two alternate design concepts incorporating more, smaller LS cells.

layers surrounding these detectors, and subjected to the same detection efficiency requirements as the above simulations (30 keVee, no gamma contamination). The lead layers started at 1" thick, and increased to 8" thick in 1" increments. The trends can be seen in figure 13. The results seem to trend as the cubed-root of the thickness for a 4" cell, as one might expect. The results for the 2" cell are more curious.

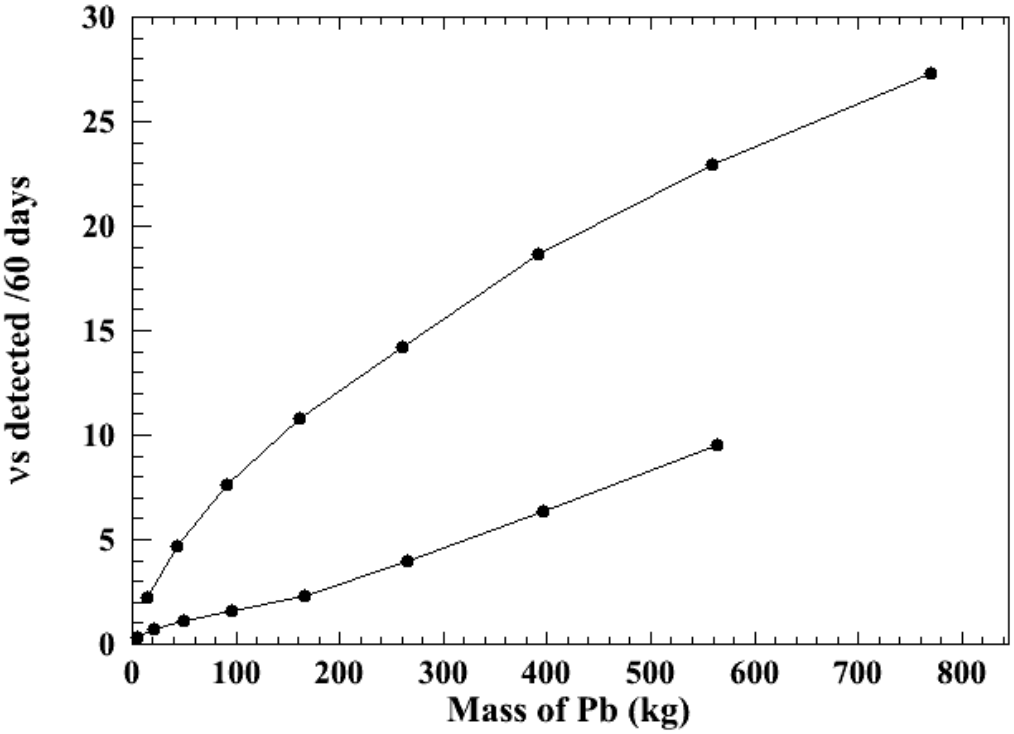

Figure 13: Neutrino event detection rates as a function of the thickness of a lead layer surrounding a 2" and 4" spherical liquid scintillator cell.

3 Optimizing the Geometric Neutron Collection Efficiency

The most promising design that we have tested so far attempts to maximize the collection efficiency of neutrons produced in the lead by surrounding the lead with liquid scintillator (instead of surrounding the liquid scintillator with lead). A conceptual drawing of this can be seen in figure 14.

3.1 Simulation

The breakdown of the individual background components can be seen in figure 15. Due to the increased collection efficiency, and improved muon veto capabilities, the expected signal now towers over the backgrounds. It is interesting to note that the μ-induced neutron spectrum appears harder than in previous geometries. This is possibly due to the proximity of the liquid scintillators to the waterbricks, and the corresponding lack of intervening material.

The liquid scintillator surrounds a 14" square brick of lead on all sides (except the bottom). The hope is that the LS cells can either be purchased in this shape, or that we can make them ourselves. PMT coverage is maximized in this design to improve the likelihood that the 30 keVee PSD threshold can be achieved.

Naively one expects $\sim$80% efficiency taking only the geometry into account. The bottom is left uncovered as it is difficult to rapidly engineer the concept with cells underneath the lead that will easily pass safety review. The cells as designed have the added advantage that they serve as the

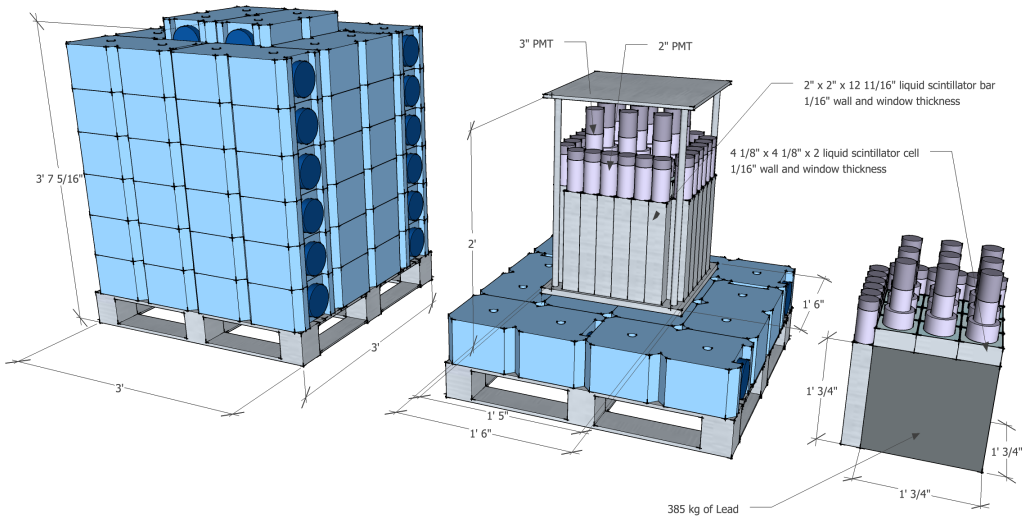

Figure 14: A design that attempts to maximize the geometric collection efficiency for neutrons produced in the Pb. The design also has the advantage that it does not need a separate muon veto surrounding the lead target, as the LS cells already serve this purpose with an estimated >99% efficiency.

muon veto for the Pb, where it is estimated to be >99%. It is conservatively assumed that there is no effect on the μ-induced neutrons from the H_2O.

3.2 Significance

With a 30 keVee threshold for efficiency n-γ PSD separation, a whipping 295 signal events can be nominally expected (in a 60 day period, 20 m from the target), on top of 122 background events (at 8 m.w.e.). This corresponds to 0.58 counts/kg Pb /60 days. The naive geometric efficiency calculation would suggest 1.05 counts/kg Pb /60 days.

The source of this discrepancy was investigated by increasing the thickness of the liquid scintillator to 3", under the assumption that neutrons were not depositing all of their energy before they escaped the cells, and thus falling below threshold. This resulted in the same 0.58 counts /kg Pb /60 days as the 2" thick cells, invalidating this hypothesis.

The geometric efficiency was able to be recovered by lowering the detector thresholds to 0 keV. The clear implication is that we have essentially maximized the geometric efficiency, and we nee do now focus on maximizing the light collection efficiency so that we can realistically achieve 30 keVee thresholds.

3.3 Concerns with Optimal Geometry

To begin with, it is not clear that the optimal n/γ separation can be achieved with long bar liquid scintillator cells. Sandia has experience deploying such detectors 20" long with double-ended PMTs. The feeling is that it may be difficult to go lower than 100 keV and that position dependent calibrations would need to be performed. On the other hand, this experience is with EJ-301, which

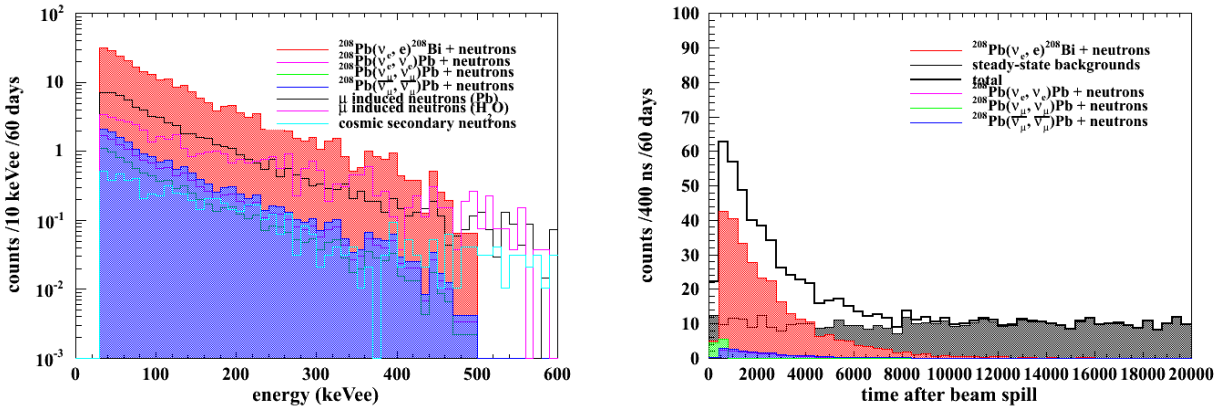

Figure 15: Expected signals and backgrounds (left) and arrival times (right) at 8 m.w.e. and 20 m from the target for the geometrically optimized geometry.

is not as good as BC-501a. Eljen has informed us that when they build liquid scintillator cells, they try to keep the ratio of the opening window to the length of the cell (for single PMT detector) below 1:4, beyond which the PSD capabilities begin to suffer.

It has been pointed out that without the lead surrounding the LS cells, they will not benefit from the shielding of the higher-than-normal level of environmental gammas[4].

To a certain extent, the presence of the water bricks serves to somewhat isolate the detector environment from any neutrons and gammas in the hallway. A very large gamma flux will contaminate the neutron signal, as some fraction of gamma interactions may be incorrectly identified as neutrons. This depends strongly on the energy of the interaction, and therefore directly effects the threshold of the experiment. The 9" of water will isolate the detector from low-energy neutrons. The experiment does, however, rely on the measurements of the higher energy neutrons that indicate that they are not present at position c5. Should higher energy neutrons be present, we risk knocking them down in energy and contaminating the signal in a difficult to simulate way.

This thickness of water will also attenuate the gammas in the environment at the level of 3.9 attenuation lengths for 100 keV gammas, and 1.13 attenuation lengths of 2 MeV gammas. This is not optimal, and thus the environmental gamma flux should probably be measured. Should it be determined that more gamma shielding is needed, it is conceivable that the low-background steel at TUNL can be used. The attenuation of a 2 MeV gamma in 1" of Steel is 0.872. This has the advantage that the expected neutron emission cross-sections in Fe are suppressed by at least an order of magnitude.

Such a design would permit us to perform a source on/off measurement by removing the lead: a convincing metric illustrating the observation of neutrinos from the source. This could prove difficult to arrange, but one could imagine building a second, lead-free pallet where the detectors could be moved into.

Another convincing metric that should probably be used, given enough statistics, is the observed decay of the excess of events with the characteristic half-life of muons (see figure 15). Such an observation may make a source on/off measurement unnecessary.

[4]As we know, this is likely due to the "nasty pipe". The rate of gammas seems to correlate with the flow rate of water through this pipe.

3.4 Optimal Geometry Design Cost Breakdown

Table 3: Cost breakdown estimate for the Optimal Geometry design.

Item	quantity	unit cost	cost
Galvanized steel pallet (4,000 lbs dyn. cap.)	1	\$169.36	\$169.36
Pb cast to shape (material & fab. cost)	1	\$600.00	\$600.00
Roof plate, 3/8" x 18" x 18" Al 7075-T6	1	\$217.08	\$217.08
Base plate, 3/4" x 18" x 18" SS	1	\$826.20	\$826.20
Inner support posts, 28", 3/4" OD, 1/4" wall th 316 SS	4	\$166.60	\$666.40
Base support posts, 7 1/2", 1" OD, 316 SS	1	\$420.00	\$420.00
Waterbricks	40	\$17.49	\$699.60
2" PMTs for LS, ETL 9266B	24	\$554.00	\$13,296.00
Voltage dividers for 2" PMTs, ETL C647	24	\$122.00	\$2,928.00
3" PMTs for LS, ETL 9265B	9	\$784.00	\$7,056.00
Voltage dividers for 3" PMTs, ETL C648	9	\$122.00	\$1,098.00
BC501a LS (unencapsulated)	32 L	\$60.47	\$1,935.00
Very Rough est. for finished cells	33 cell	∼\$500 /cell	∼\$16,500.00
Digiters & Electronics (Duke & ORNL? & ...)	-	-	-
total construction and material costs			\$44,468.64
cost /ν /1 yr			\$24.76